DNA AND CELL BIOLOGY
Volume 39, Number 2, 2020

Pp. 310–320
DOI: 10.1089/dna.2019.4966

Aerobic Endurance Exercise Ameliorates Renal Vascular Sclerosis in Aged Mice by Regulating PI3K/AKT/mTOR Signaling Pathway

Chuncha Bao,[1] Zhong Yang,[2] Qian Li,[1] Qiyan Cai,[3] Hongli Li,[3,*] and Bin Shu[1,*]

Renal vascular sclerosis caused by aging plays an important role in the occurrence and development of chronic kidney disease. Clinical studies have confirmed that endurance exercise is able to delay the aging of skeletal muscle and brain tissue. However, to date, few studies have assessed whether endurance exercise is able to improve the occurrence of renal vascular sclerosis caused by natural aging and its related mechanisms. In this study, we investigated the protective effect of aerobic endurance exercise on renal vascular sclerosis in aged mice and its effect on the phosphatidylinositol 3-kinase/protein kinase B/mammalian target of rapamycin (PI3K/AKT/mTOR) pathway. The results suggested that aerobic endurance exercise preserved kidney morphology and renal function. Glomerular basement membrane thickness was evidently increased, podocyte foot processes were effaced in aged mice, and aerobic endurance exercise significantly ameliorated the overall lesion range. The protein expression of vascular endothelial growth factor (VEGF) and JG12 was lower in the senile control group (OC group). The protein expression of VEGF and JG12 was significantly increased after aerobic endurance exercise. Furthermore, aerobic endurance exercise resulted in downregulation of Bax, Caspase 3, IL-6, and senescent cells and upregulation of Bcl-2. The upregulation of PI3K and its downstream signal molecules AKT and mTOR after aerobic endurance exercise was further observed. Our observations indicated that aerobic endurance exercise may inhibit renal vascular sclerosis in aged mice by regulating the PI3K/AKT/mTOR signaling pathway.

Keywords: aging, renal vascular sclerosis, aerobic endurance exercise, PI3K/AKT/mTOR, apoptosis

Introduction

Increasing evidence has confirmed that renal vascular sclerosis caused by aging plays an important role in the occurrence and development of chronic kidney disease (Osullivan *et al.*, 2017). Previous studies have indicated that the viability of microvascular endothelial cells in senile kidney tissue decreased, suggesting that there might be disorder in the angiogenesis of renal tissue with age (Satoh *et al.*, 2013; Barton, 2014). Therefore, it is of great significance to study the capillary structure of the kidney and the role of vascular endothelial cells in the progression of kidney disease for the prevention and treatment of chronic kidney disease. At this time, there is no effective pharmacological intervention that prevents or attenuates the occurrence and development of chronic kidney disease.

However, studies have indicated that aerobic exercise training is an important means of rehabilitation, which may effectively prevent chronic diseases and delay aging (Viña *et al.*, 2016; Yuho *et al.*, 2017). Meanwhile, previous studies have demonstrated that exercise is able to improve vascular function (Nyberg *et al.*, 2012; Gliemann *et al.*, 2018). However, whether exercise may improve the vascular function caused by natural aging requires further investigation.

In the process of aging, the function of vascular endothelial cells disorders, progressively reduces, and loses. The loss of microvascular endothelial cells is mainly linked to the decrease of endothelial cell repairability, the decrease of proliferation, and the increase of apoptosis (Collett *et al.*, 2017; Papazova *et al.*, 2018). The angiogenesis is mainly dependent on vascular endothelial growth factor (VEGF), an important survival factor of endothelial cells, which is closely linked to renal microangiogenesis and has an important role in the proliferation, differentiation, and survival of endothelial cells (Ferrara *et al.*, 2001, 2003; Majumder and Advani, 2016). JG12 is considered to be a good marker of

[1]Department of Rehabilitation Medicine, University-Town Hospital, Chongqing Medical University, Chongqing, China.
Departments of [2]Clinical Blood Teaching and Research and [3]Histology and Embryology, Army Medical University, Chongqing, China.
*These authors contributed equally to this article.

vascular endothelial cells (Li, 2012). Bragana *et al.* (de Bragança, 2018) demonstrated that the process of moderate chronic kidney disease in five of six nephrectomy rats (Nx) is followed with renal vascular sclerosis and lower expression of JG12 protein.

Apoptosis, a well-studied programmed cell death and catabolic system, is critical for tissue development and homeostasis. A growing body of evidence supported that elevated vascular dysfunction is based on increased cellular inflammatory response and apoptosis (Pope *et al.*, 2016; Ghosh *et al.*, 2017). High levels of diverse proinflammatory cytokines such as interleukin-6 (IL-6) (Arida *et al.*, 2018) were observed consistently in human-associated atherosclerotic study. Another study has demonstrated that apoptosis of human umbilical vein endothelial cells is closely related to the upregulation of Bax/Bcl-2 and Caspase 3 expression levels (Wu *et al.*, 2016). Notably, the phosphatidylinositol 3-kinase/protein kinase B/mammalian target of rapamycin (PI3K/AKT/mTOR) signaling pathway is closely linked to various cell activities, including cell metabolism, growth, migration, and proliferation (Chen *et al.*, 2017; Ye *et al.*, 2018; Zhang *et al.*, 2018). Furthermore, the PI3-K/AKT/mTOR signaling pathway plays an important role in regulating apoptosis. For instance, Shao *et al.* (2017) found that the PI3K inhibitor is able to decrease the expression of pro-apoptotic proteins (Caspase 3, Bax).

In addition, the activation of the PI3K/AKT/mTOR/signaling pathway is closely linked to the upregulation of VEGF for angiogenesis (Wang *et al.*, 2014; Zhu *et al.*, 2016). For instance, the silencing of VEGF inhibits cell proliferation and promotes cell apoptosis by downregulating the PI3K/AKT signaling pathway (Yan *et al.*, 2019). To date, the study by Schnell *et al.* (Schnell, 2008; Karar, and Maity, 2011) confirmed that NVP-BEZ235, which is a dual PI3K and mTOR inhibitor, blocked VEGF-induced neovascularization in rats. Wang *et al.* (2011) demonstrated that the VEGF/Flt-mediated migration of AG1-G1-Flt1 cells (hemangioma endothelial cells were established from a human angioma) occurred mainly via the activation of the PI3K/AKT pathway. Therefore, these prior studies indicated that the PI3K/AKT/mTOR signaling pathway is related to the renal vascular dysfunction caused by apoptosis.

This research, for the first time, studied the effects of aerobic endurance exercise on renal vascular sclerosis in aged mice and its related mechanisms. Therefore, the purpose of the present study was to compare and observe whether aerobic endurance exercise leads to an improvement of renal vascular aging through subjecting aged mice to aerobic endurance exercise. In addition, it further clarifies whether the underlying mechanisms include the P13K/AKT/mTOR signaling pathway and induction of apoptotic protein activation. In a broader context, our findings will provide molecular experimental evidence for aerobic endurance exercise to prevent and treat renal vascular sclerosis.

Materials and Methods

Experimental animals

A total of 45 healthy male C57/BL mice (19-month-old, $n=30$ and 2-month-old, $n=15$) were purchased from the Laboratory Animal Breeding and Research Center, Army Military Medical University, China (license no. SYXK-PLA-20120031). All surgical procedures were approved by the Laboratory Animal Welfare and Ethics Committee of the Third Military Medical University. All animals were housed in standard rodent cages at a temperature 20 ± 5°C, ventilation- and light-controlled (12:12 h light–dark cycle) environment, and fed with a standard diet of pellets and clean tap water. Laboratory animal bedding materials were renewed once a week; the drinking bottles were sterilized daily.

Animal groups and exercise training

The 45 healthy male C57/BL mice were divided into three groups: young control group (YC group, 2-month-old, $n=15$), senile control group (OC group, 19-month-old, $n=15$), and senile exercise group (OY group, 19-month-old, $n=15$). Aged mice underwent the rotatable treadmill training in the same room where the animals were kept. Conducting a week of adaptability training, animals have an interval of a week before the beginning of training program, at the end of which we do it according to the training program, 5 day/week, and lasted for 6 weeks. The load was gradually increased (low-intensity activities refers to the movement speed within 10 m/min and training intensity of 30–40% VO2 max) (Marcaletti and Feige, 2011; Roof *et al.*, 2015). Within 24 h after the end of exercise training, all mice were euthanized by cervical dislocation. Some kidney tissues were fixed with neutral formaldehyde, and the rest were frozen rapidly in liquid nitrogen. The training program is shown in Table 1 (Bellafiore *et al.*, 2007; Chimenti *et al.*, 2007).

Detection for renal function

Within 24 h after the end of exercise training, blood samples were obtained from the tail veins, centrifugations of blood samples were performed, and the serums were stored at −20°C. The blood urea nitrogen (BUN), uric acid (UA), and serum creatinine (Scr) were measured by an AutoAnalyzer with BUN (cat. no. JL20491; Jianglai Biological Technology, Shanghai, China), UA (cat. no. JL20492; Jianglai Biological Technology), and Scr test kits (cat. no. JL20633; Jianglai Biological Technology) (Zhu *et al.*, 2016).

Hematoxylin and eosin staining

Samples of kidney tissues were sectioned by 4 μm. Then, the sections were dewaxed with xylene and dehydrated through a graded series of alcohol. The sections were stained with hematoxylin (CAT Hematoxylin) for 5 min. After rinsing in distilled water three times for 5 min, the sections were

Table 1. Weeks of Exercise, Session Time, Rotations, Length, and Speed Used for Training Program

Week	*Session time (min)*	*Rotations (/min)*	*Length (m)*	*Speed (m/min)*
1	15	16	48	3.2
2	30	16	96	3.2
3	30	20	120	4
4	45	20	180	4
5	60	20	240	4
6	60	24	288	4.8

stained with eosin for 3 min. The sections were observed under a light microscope at ×200 magnification.

Periodic acid–Schiff staining

The kidney tissue slices were dehydrated through a graded series of ethanol. The sections were incubated with oxygenant for 8 min and then washed in distilled water three times for 5 min per wash. The sections were stained with Schiff's solution for 20 min. After rinsing in distilled water for 10 min, dye cell nucleus with hematoxylin and gradient dehydration were applied before mounting with neutral gum. Pathological changes of the kidney tissues in mice were observed under an inverted microscope (BX60; Olympus, China). The percentage of renal vascular sclerosis was determined as the red area divided by the area of the entire field, and the average optical density (OD value) was calculated using Image-Pro Plus 6.0 image analysis software (version 6.0; Media Cybernetics, Inc., MD).

Transmission electron microscope

The kidney tissues were diced into proper size (1 mm^3) and fixed by immersion in 3% buffered glutaraldehyde for 10–12 h at 4°C. Then, tissue specimens were fixed in 1% osmium tetroxide in cacodylate buffer (pH 7.2) for 90 min at 30°C. The dehydration of fixed tissues was carried out with ascending grades of ethanol, and then, the tissues were transferred to epoxy resin via propylene oxide. Semi-thin sections were prepared for the purpose of tissue orientation and stained with toluidine blue. Ultra-thin sections (60 nm) were cut on an ultra-microtome and stained with uranyl acetate and lead citrate. Stained sections were observed under the transmission electron microscope (TEM, HT7800; Hitachi, Japan).

Senescence-associated β-galactosidase assay

Kidney specimens were embedded in optimum cutting temperature compound, frozen in acetone dry ice mixture, and cut into 10 μm sections on a cryostat. Sections were socked and fixed in 1 mL beta-galactosidase staining stationary solution at room temperature for 30 min. Then, the kidney tissues were washed three times with phosphate-buffered saline (PBS) for 5 min per wash. The kidney tissues were incubated overnight with appropriate amount of dyeing working liquid at 37°C. Senescent-positive products of the kidney tissues in mice were observed under an inverted microscope (BX60; Olympus). The average OD value was calculated using Image-Pro Plus 6.0 image analysis software (version 6.0; Media Cybernetics, Inc.).

Reverse Transcription PCR

Total RNA of the kidney tissues was shattered by ultrasonic crusher after adding TRIzol reagent (Life Technology, Carlsbad, CA) (Zhao *et al.*, 2015). The purity and concentration of extracted RNA were detected by micronuclei acid protein analyzer. The extracted RNA was reverse transcribed into cDNA using a PrimeScript™ RT-PCR Kit (Takara, Tokyo, Japan) according to the manufacturer's instructions. PCR amplification was performed using Ex Taq (Takara) in a final reaction volume of 20 μL (C1000 Touch™ Thermal Cycler; Bio-Rad). The amplification protocol was as follows: predenaturation at 94°C for 5 min, denaturation at 94°C for 30 s, and renaturation at 55°C for 30 s (35 cycles). The amplified products were detected in agarose gel electrophoresis. Then, the gray scale of PCR band was calculated (normalized with those of β-actin) via Image-Pro Plus image analysis system (version 6.0; Media Cybernetics, Inc.). The primers used for examining the expression were shown in Table 2.

Immunohistochemical staining

The kidney tissue sections were deparaffinized with xylene and dewaxed, and then, heat-mediated antigen retrieval was performed by microwaving for 20 min in sodium citrate. After rinsing in PBS three times for 5 min and exhaustion of endogenous peroxidase with methanol and hydrogen peroxide for 30 min at room temperature, the sections were blocked with 0.5% bovine serum albumin for 1 h at 37°C and incubated with JG12 (cat. no. sc-65390; Santa Cruz Biotechnology, CA) overnight at 4°C. The sections were washed three times with PBS for 5 min per wash and then incubated with the rabbit anti-mouse antibody (cat. no. SA1026; Boster Biological Technology, China) at 37°C for 1 h. Diaminobenzidine (DAB) was used for visualization (Cai *et al.*, 2014). The specimens were then counterstained with hematoxylin, xylene transparent. The neutral resin sealing was used for sealing. Lung tissue sections used as positive controls were put through the same procedure. The positive controls refer to the antibody manual; there are positive reactions in the positive controls. Negative controls were put through the same procedure after PBS was used to replace the primary antibody; all negative controls lacked a positive reaction. Tissue sections were observed and photographed with a microscope (BX60; Olympus). Image-Pro Plus 6.0 image analysis software was used to automatically analyze the images and calculate the OD value.

Immunofluorescence staining

The kidney tissue sections were incubated with VEGF (cat. no. AF0312; Shanghai Beyotime Biotech, China), p-AKT (cat. no. ab81283; Abcam), and p-mTOR (cat. no. ab84400;

Table 2. Primer Sequences Utilized in This Study

Gene name	*Forward primer (5′–3′)*	*Reverse primer (5′–3′)*
Caspase 3	5′-GAAACTCTTCATCATTCAGGCC-3′	5′-GCGAGTGAGAATGTGCATAAAT-3′
IL-6	5′-CTCCCAACAGACCTGTCTATAC-3′	5′-CCATTGCACAACTCTTTTCTCA-3′
Bax	5′-CCGCCGTGGACACAGAC-3′	5′-CAGAAAACATGTCAGCTGCCA-3′
Bcl-2	5′-TCCGATCAGGAAGGCTAGAGTT-3′	5′-TCGGTCTCCTAAAAGCAGGC-3′
β-Actin	5′-GTGACGTTGACATCCGTA-3′	5′-GTAACAGTCCGCCTA-3′

Abcam) overnight at 4°C. The PBS buffer was washed thoroughly three times for 5 min per wash and then incubated with fluorescently labeled mouse anti-rabbit IgG-FITC (sc-2359; Santa Cruz Biotechnology) at 37°C for 2 h (protection from light) (Cai *et al.*, 2014). After rinsing in PBS three times for 5 min per wash, the cell nuclei were stained with the Hochest (cat. no. sc-200908; Santa Cruz Biotechnology). The positive controls of VEGF, p-AKT, and p-mTOR correspond to lung carcinoma tissue, cervical carcinoma tissue, and hippocampus tissue. All the above positive controls refer to the antibody manual. Positive controls were put through the same procedure; there are positive reactions in the positive controls. Negative controls were put through the same procedure after PBS was used to replace the primary antibody; all negative controls lacked a positive reaction. The images were taken by laser scanning confocal microscope (FluoView™ FV1000; Shanghai, China). Image-Pro Plus 6.0 image analysis software was used to automatically analyze and calculate the OD value.

Western blot

The total kidney tissues were obtained by homogenization in a tissue protein extraction reagent (Radio Immunoprecipitation Assay lysis buffer [RIPA] lysis buffer; Millipore, Billerica, MA) supplemented with complete protease inhibitors. The lysate was centrifuged (12,000 × *g*) at 4°C for 10 min and the supernatant was used. Total protein concentrations were determined using a Bicinchoninic Acid Protein Assay Kit (Thermo Fisher Scientific). After boiling for 10 min in loading buffer, the protein tissue lysates were separated by electrophoresis on 10% sodium dodecyl sulfate–polyacrylamide gel electrophoresis (SDS-PAGE), followed by transfer of proteins to polyvinylidene difluoride (PVDF) membranes. The PVDF membranes were blocked with 1% nonfat dried milk in 10 mM tris-buffered saline (TBS) with 0.05% Tween-20 (TBST) for 1 h. The PVDF membranes were sequentially incubated with the following primary antibodies: JG12 (cat. no. sc-65390; Santa Cruz Biotechnology), VEGF (cat. no. AF0312; Shanghai Beyotime Biotech), AKT (cat. no. ab81283; Abcam), p-AKT (cat. no. ab38449; Abcam), mTOR (cat. no. ab2732; Abcam), p-mTOR (cat. no. ab131538; Abcam), Cleaved-Caspase 3 (cat. no. ab2302; Abcam), and GAPDH (cat. no. AF0006; Shanghai Beyotime Biotech) at a dilution of 1:1000 overnight at 4°C. The membranes were washed with TBST three times for 10 min per wash and incubated with mouse anti-rabbit immunoglobulin-Horseradish peroxidase [IgG-HRP] labeling (cat. no. sc2357; Santa Cruz Biotechnology) and rabbit anti-mouse IgG-HRP (cat. no. sc358914; Santa Cruz Biotechnology) for 2 h at room temperature. The protein blots were visualized using Enhanced Chemiluminescence Western Blotting Luminol Reagent (GE Healthcare). All protein blots were quantified using Image-Pro Plus 6.0 image analysis software (Media Cybernetics, Inc.).

Statistical analysis

All data from experiments are expressed as the mean ± standard deviation. We used one-way analysis of variance to analyze differences among groups. Tukey's *post hoc* test was performed using SPSS 22.0 (IBM, Armonk, NY). The positive areas were evaluated by integrated OD value and analyzed using Image-Pro Plus 6.0. A p-value <0.05 was considered to be statistically significant.

Results

Aerobic endurance exercise improves renal function parameters in aged mice

The results from kidney function demonstrated that the BUN ($p < 0.01$), Scr ($p < 0.01$), and UA levels ($p < 0.05$) were significantly increased in the OC group compared with those in the YC group. Aerobic exercise training reduced the BUN, Scr, and UA levels ($p < 0.05$) compared with those in the OC group (Fig. 1A–C).

Aerobic endurance exercise improves pathological morphology of kidney tissues in aged mice

Hematoxylin and eosin (H&E) staining suggested that in the OC group, reduction of glomerular volume and unclear glomerular structure were observed. The number of epithelial cells in glomeruli and tubules decreased significantly. In the YC group, the glomerular structure was clear, basement membrane was intact, and cell morphology was normal. The number of epithelial cells in glomeruli and tubules increased significantly. In the OY group, normal glomerular structure was observed, and there was no obvious glomerular atrophy (Fig. 2A). In periodic acid–Schiff (PAS)

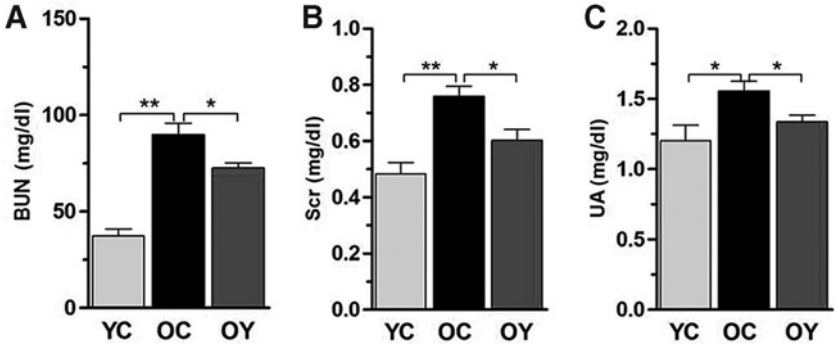

FIG. 1. BUN, Scr, and UA levels were detected using vein blood samples in three groups. **(A–C)** BUN, Scr, and UA levels were increased in renal artery of aged mice compared with young mice. Aerobic exercise decreased BUN, Scr, and UA levels of renal artery in the senile control group (OC group). The values represent the mean ± SD ($n = 5$). *$p < 0.05$, **$p < 0.01$. BUN, blood urea nitrogen; Scr, serum creatinine; SD, standard deviation; UA, uric acid.

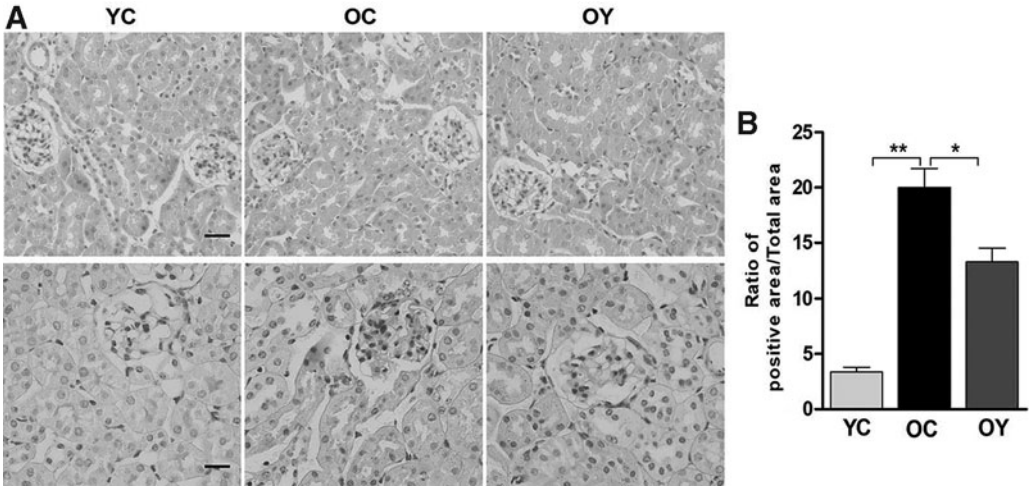

FIG. 2. Effect of aerobic endurance exercise on kidney histological morphology changes. **(A)** Kidney stained with hematoxylin and eosin and periodic acid–Schiff from the young control group (YC group), the senile control group (OC group), and the senile exercise group (OY group) (400×), scale bar, 50 μm. **(B)** The quantitative results showing the degree of damage between different groups. The values represent the mean ± SD ($n = 5$). *$p < 0.05$, **$p < 0.01$.

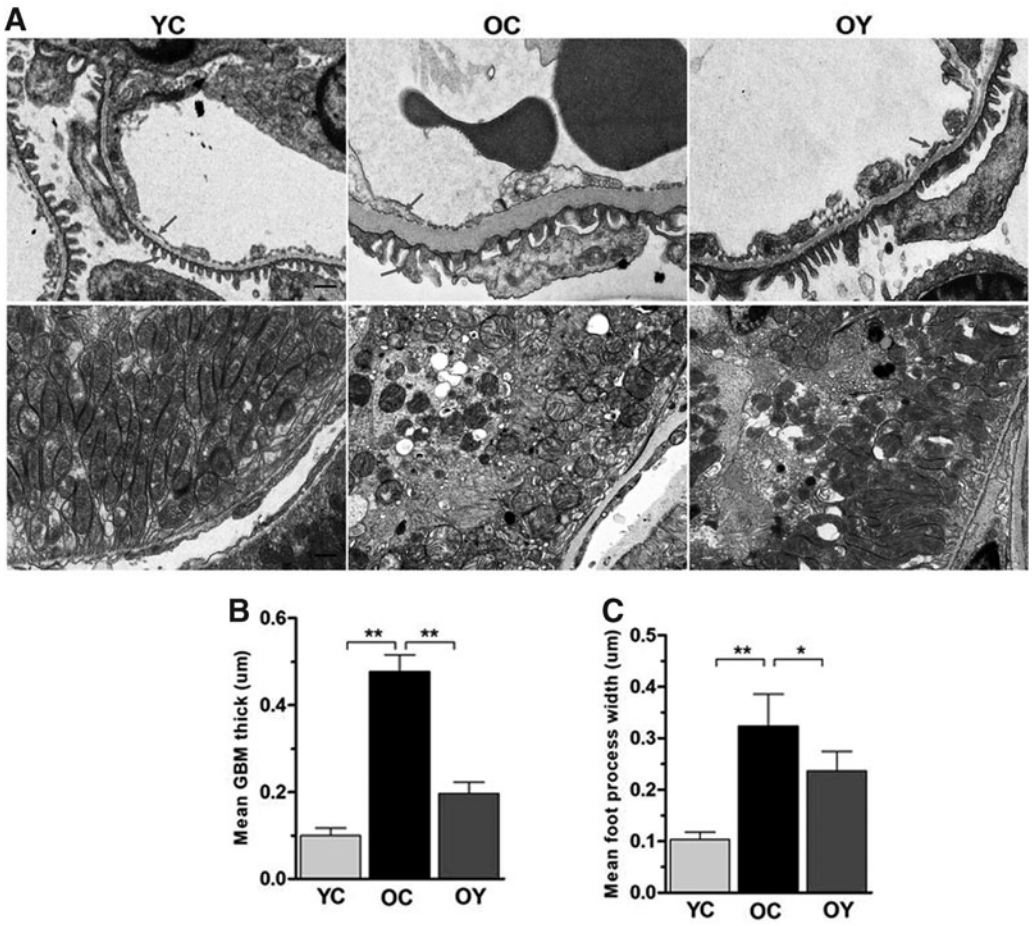

FIG. 3. Effect of aerobic endurance exercise on podocyte ultrastructural alterations. **(A)** Representative TEM photomicrographs showing the GBM thickness, foot processes open slit pores, and mitochondrial cristae (*arrows*); magnification, ×6k, ×12k; scale bar, 1 μm. **(B, C)** Quantifications of the mean GBM thickness and the mean foot processes width in podocytes from the three groups. The values represent the mean ± SD ($n = 5$). *$p < 0.05$, **$p < 0.01$. GBM, glomerular basement membrane; TEM, transmission electron microscope.

staining, the regions of purple-red staining represent glycogen. The positive products increased significantly in the OC group compared with those in the YC group ($p < 0.01$), and compared with those in the OC group, the positive products decreased significantly after aerobic endurance exercise ($p < 0.05$) (Fig. 2B).

The results from TEM demonstrated that within the YC group, the glomerular basement membrane (GBM) thickness was normal and the structure was clear, in which the dense layer and transparent layer were also clear. The podocyte foot processes were arranged neatly, and mitochondrial cristae of proximal tubular epithelial cells were apparent. Within the OC group, the GBM thickness was evidently increased and the podocyte foot processes were effaced. The gap between the two podocyte foot processes was significantly widened, and proximal tubular epithelial cells mitochondrial cristae were not apparent or disappeared. In contrast, aerobic endurance exercise significantly ameliorated the overall lesion range (Fig. 3A). Specifically, the GBM thickness and foot process width were increased in the OC group compared with those in the YC group ($p < 0.01$) (Fig. 3B, C). After aerobic endurance exercise, the GBM thickness ($p < 0.01$) and podocyte foot processes ($p < 0.05$) were decreased compared with those in the OC group.

Effects of aerobic endurance exercise on the expression of glomerular vascular endothelial cell markers in aged mice

Analysis of western blot indicated that the protein expression levels of VEGF and JG12 in the OC group were significantly lower than those in the YC group ($p < 0.01$). In addition, aerobic endurance exercise increased the protein expression levels of VEGF and JG12 compared with those in the OC group ($p < 0.05$) (Fig. 4A–C). In the OC group, there were only slight VEGF- and JG12-positive signals in glomeruli, whereas there were higher expression levels of VEGF and JG12 in the YC group compared with those in the OC group. In the OY group, the VEGF- and JG12-positive signals were weaker than those in the YC group but higher than those in the OC group (Fig. 4D). The results suggested that the expression levels of VEGF and JG12 were significantly lower in the OC group compared with those in the YC group ($p < 0.01$). After aerobic endurance exercise, the expression levels of VEGF and JG12

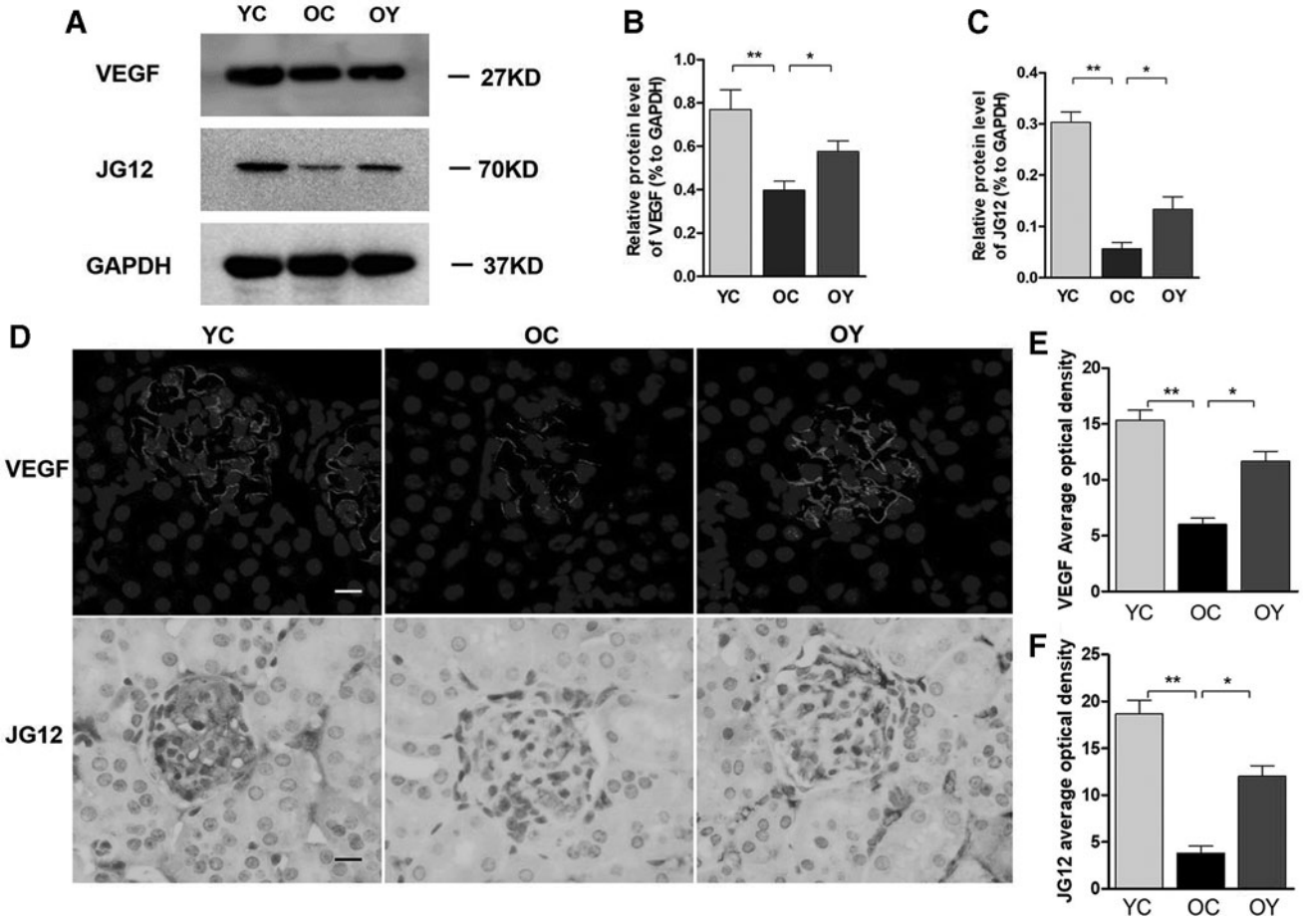

FIG. 4. Effects of aerobic endurance exercise on the expression of the VEGF and JG12 in the kidney tissues of aged mice. **(A)** Western blot analysis showed VEGF and JG12 protein expression changes in the three groups. **(B)** Relative quantification of VEGF and **(C)** JG12 is depicted in *bar graphs*. The values represent the mean ± SD ($n = 3$). *$p < 0.05$, **$p < 0.01$. **(D)** VEGF and JG12 expression was identified by immunofluorescence staining; magnification, ×400; scale bar, 50 μm; represent positive signal. **(E)** Relative OD value of VEGF and **(F)** JG12 staining is depicted in *bar graphs*. The values represent the mean ± SD ($n = 5$). *$p < 0.05$, **$p < 0.01$. OD, optical density; VEGF, vascular endothelial growth factor.

in glomeruli of the OY group were significantly higher than those of the OC group ($p < 0.05$) (Fig. 4E, F). Therefore, our results reinforced the important role of aerobic endurance exercise on the amelioration of endothelial function.

Effects of aerobic endurance exercise on the activity of the PI3K/AKt/mTOR signaling pathway in aged kidney

Senescence and apoptosis of vascular endothelial cells involve the activation of the PI3K/AKT/mTOR pathway. The results of western blot analysis indicated that the expression levels of PI3K, p-AKT/AKT, and p-mTOR/mTOR were significantly lower in the OC group compared with those in the YC group ($p < 0.01$) and were markedly upregulated in the OY group compared with those in the OC group ($p < 0.05$) (Fig. 5C–E). Immunofluorescence revealed that the OD value of the p-AKT- and p-mTOR-positive signals was significantly higher in the YC group compared with those in the OC group ($p < 0.01$), and aerobic endurance exercise significantly increased the OD value of the p-AKT- ($p < 0.05$) and p-mTOR ($p < 0.01$)-positive signals, which differed significantly from those in the OC group (Fig. 5F, G).

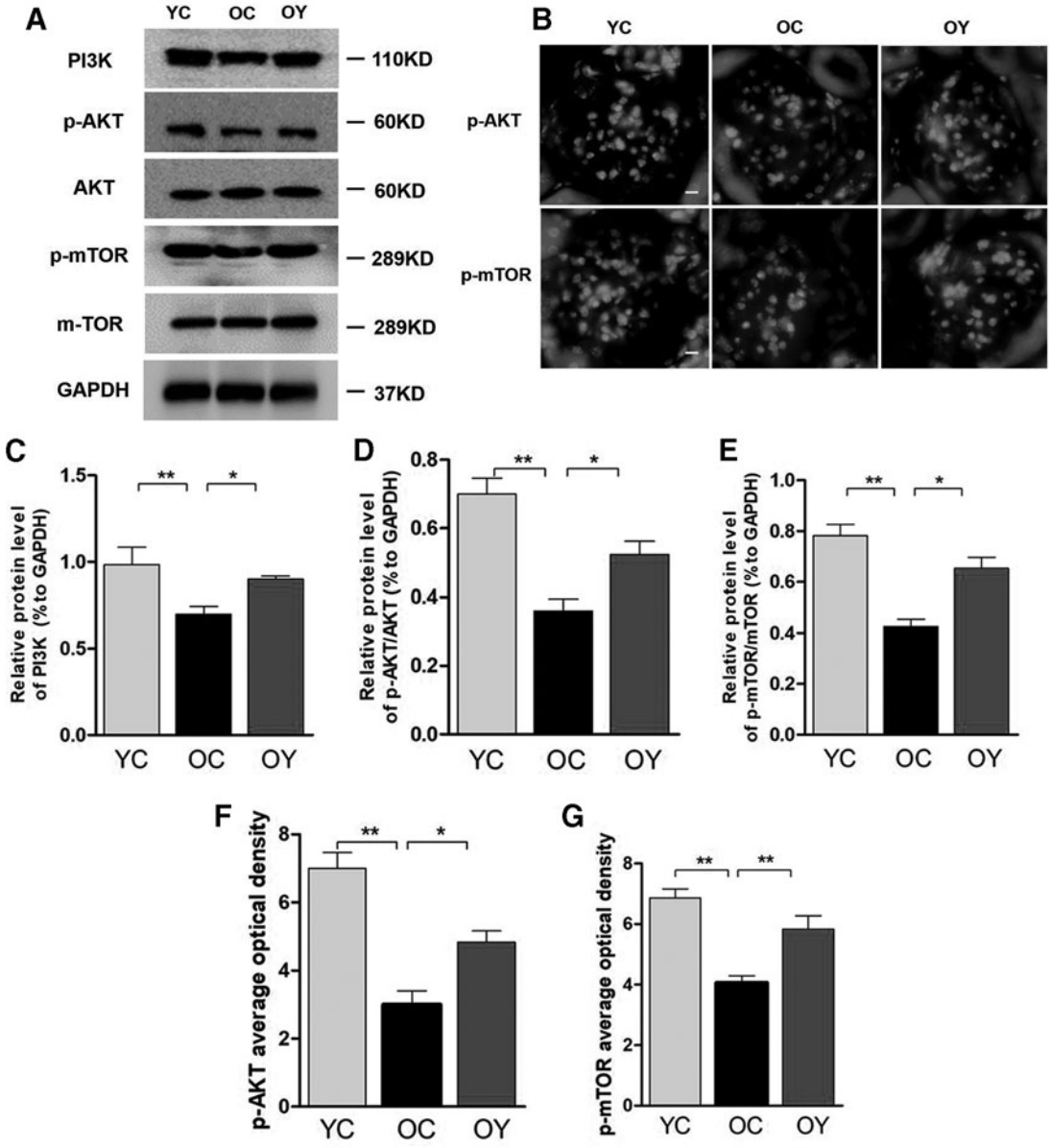

FIG. 5. Effects of aerobic endurance exercise on expression of the PI3K/AKT/mTOR pathway in the kidney tissues of aged mice. **(A)** Western blot analysis showed PI3K, p-AKT/AKT, and p-mTOR/mTOR protein expression changes in the three groups. **(B)** p-AKT and p-mTOR expression was identified by immunofluorescence staining; magnification, ×400; scale bar, 50 μm. **(C–E)** Relative quantification of PI3K, p-AKT/AKT, and p-mTOR/mTOR is depicted in *bar graphs*. The values represent the mean ± SD ($n = 3$). *$p < 0.05$, **$p < 0.01$. **(F)** Relative OD value of p-AKT staining are depicted in bar graphs. The values represent the mean ± SD. ($n = 5$). *$p < 0.05$, **$p < 0.01$. **(G)** Relative OD value of p-mTOR staining are depicted in bar graphs. The values represent the mean ± SD. ($n = 5$). **$p < 0.01$. PI3K/AKT/mTOR, phosphatidylinositol 3-kinase/protein kinase B/mammalian target of rapamycin.

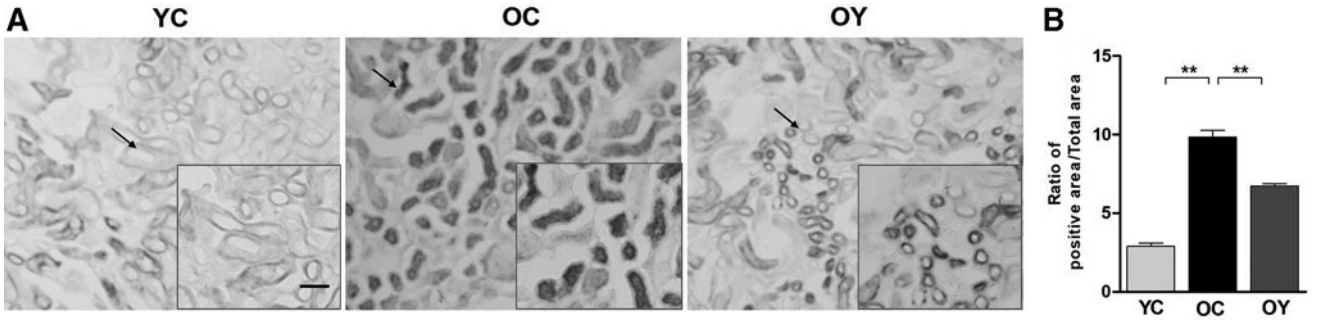

FIG. 6. Senescence β-galactosidase staining to observe senescence in the kidney tissues of aged mice. **(A)** Senescence β-galactosidase staining of the three groups; magnification, ×400; scale bar, 50 μm. **(B)** The quantitative results showing the percentages of senescence between different groups. The values represent the mean ± SD ($n = 5$). $^{**}p < 0.01$.

Aerobic endurance exercise delays kidney tissue senescence

To determine the role of aerobic endurance exercise on kidney tissue senescence, we measured senescence-associated β-galactosidase (SA-β-gal) activity of kidney tissue, a representative feature of senescence. The blue-positive products were significantly increased in the OC group compared with those in the YC group. Compared with the OC group ($p < 0.01$), the positive products were significantly decreased after aerobic endurance exercise, but the ratio was still higher than those in the YC group ($p < 0.01$) (Fig. 6A, B).

Effects of aerobic endurance exercise on the expression of apoptotic and inflammatory markers in aged kidney

Reverse Transcription (RT)-PCR results showed that *Caspase 3* mRNA, *IL-6* mRNA, and *Bax* mRNA expression levels were significantly increased in the OC group compared with those in the YC group ($p < 0.01$). After aerobic endurance exercise, the *Caspase 3* mRNA, *IL-6* mRNA, and *Bax* mRNA expression levels were lower than those in the OC group ($p < 0.05$) (Fig. 7A–D). However, *Bcl-2* mRNA showed an opposite trend; the *Bcl-2* mRNA expression level

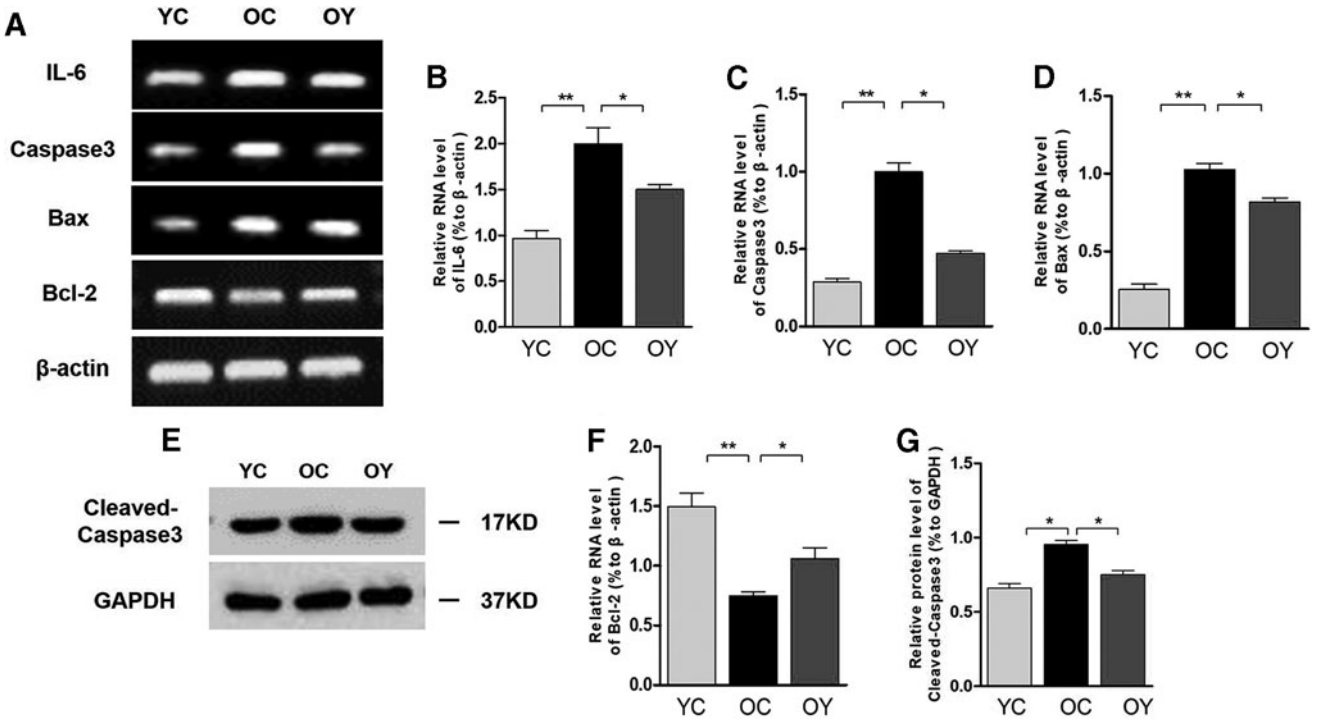

FIG. 7. Effects of aerobic endurance exercise on Caspase3, *IL-6* mRNA, *Bax* mRNA, and *Bcl-2* mRNA expression in the kidney tissues of aged mice. **(A)** RT-PCR analysis showed *Caspase3* mRNA, *IL-6* mRNA, *Bax* mRNA, and *Bcl-2* mRNA expression changes in the three groups. **(B–D)** Relative quantification of *Caspase3* mRNA, *IL-6* mRNA, and *Bax* mRNA is depicted in *bar graphs*. The values represent the mean ± SD ($n = 3$). $^{*}p < 0.05$, $^{**}p < 0.01$. **(E)** Western blot analysis showed Cleaved-Caspase3 protein expression changes in the three groups. **(F)** Relative quantification of *Bcl-2* is depicted in *bar graphs*. The value represent the mean ± SD ($n = 3$). $^{*}p < 0.05$, $^{**}p < 0.01$. **(G)** Relative quantification of Cleaved-Caspase3 is depicted in *bar graphs*. The values represent the mean ± SD ($n = 3$). $^{*}p < 0.05$.

in the OC group was significantly lower than that in the YC group ($p < 0.01$). After aerobic endurance exercise, the *Bcl-2* mRNA expression level was higher than that in the OC group ($p < 0.05$) (Fig. 7F). In addition, the protein expression level of Cleaved-Caspase 3 in the OC group was significantly higher than that in the YC group ($p < 0.05$). After aerobic endurance exercise, the protein level of Cleaved-Caspase 3 was decreased compared with that in the OC group ($p < 0.05$) (Fig. 7G).

Discussion

Aging is both a natural and ineluctable biological process. With advancing age, the kidneys undergo physiological and pathological changes, such as interstitial fibrosis, tubular atrophy, glomerular vascular sclerosis, basement membranes thickening, and cells aging (Glassock and Rule, 2012; Denic *et al.*, 2016; Hommos *et al.*, 2017). To better understand the relationship between aging and renal vascular sclerosis, in the present study, detection for renal function was used to observe 2-month-old and 19-month-old mice, and the results demonstrated that aging damages renal function as evidenced by increased levels of BUN, UA, and Scr. H&E and PAS staining further revealed glomerular atrophy, increased cytolysis, and massive deposition of glycogen in aged mice, indicating obvious glomerulosclerosis in the kidney tissues of aged mice, which were consistent with the results of previous studies. Furthermore, the results from TEM demonstrated that GBM thickness was significantly increased, as well as podocyte foot processes were effaced in the OC group compared with those in the YC group, indicating that renal vascular sclerosis of aged mice is consistent with the results of previous studies.

Exercise is an effective rehabilitation method for delaying aging, which may improve the function of the brain and kidney tissues in aging rats (Garatachea *et al.*, 2015; Banks, 2016; Rzechorzek, 2017). Luan *et al.* (Ji *et al.*, 2018) indicated that aerobic exercise induced upregulation of Klotho to extend life span by attenuating the excess production of reactive oxygen species in the brain and kidney. At the same time, studies have demonstrated that exercise is able to improve endothelial function in the elderly patients with chronic kidney disease (Martens, 2016). Whether exercise may improve renal vascular sclerosis caused by natural aging is rarely studied. In this study, 15 aged mice were trained with rotarod treadmill endurance exercise for 6 weeks, and the results of H&E and PAS staining demonstrated that aerobic endurance exercise improves pathological morphology of kidney tissues in aged mice. Additionally, TEM indicated that aerobic endurance exercise significantly ameliorated the overall lesion range of kidney, GBM thickness was decreased, there was less fading of the podocyte foot processes, and the number of open slit pores was increased compared with those in the OC group, suggesting that aerobic endurance exercise is able to improve renal vascular sclerosis of aged mice.

The development of glomerulosclerosis is closely linked to the loss of glomerular capillaries; one of the important features of vascular aging is endothelial dysfunction (Brodsky *et al.*, 2004). An *in vitro* and preclinical data supported that the aging-induced oxidative stress results in the decrease of NOS expression and the impairment of endothelium-dependent vasodilation (Bhayadia *et al.*, 2016). VEGF is an important angiogenic factor, which is able to stimulate the proliferation of vascular endothelial cells, increase the permeability of endothelial cells, and participate in angiogenesis (Del *et al.*, 1999). JG12 is a specific marker for the vascular endothelium, which is only expressed on the surface of the capillary endothelium. In this study, the results suggested that the positive signals of VEGF and JG12 in the YC group were strong and were uniformly expressed at high levels in glomerulus. Furthermore, the positive signal of VEGF and JG12 in the OC group was weak. However, the expression of VEGF and JG12 protein in glomeruli of the endurance exercise group was higher than that of the non-exercise group, suggesting that aerobic endurance exercise is able to improve the function of vascular endothelial cells in the kidney tissues of aged mice.

Blood vessel aging is closely linked to senescence and apoptosis of endothelial cells. In the current study, SA-β-gal staining revealed that senescent cells in aged kidney were reduced after aerobic endurance exercise. In addition, apoptosis usually involves increasing apoptotic proteins (such as Bax and Caspase 3) and decreasing the expression of anti-apoptotic proteins (Bcl-2) (Tian *et al.*, 2016). Preclinical studies have indicated that the expression of Bax, Caspase 3, and IL-6 was increased after renal capillary injury induced by diabetes mellitus, suggesting that IL-6, Caspase 3, and Bax play an important role in renal vascular aging (Yu *et al.*, 2017). Our results also revealed that the mRNA levels of Caspase 3 and Bax in the OC group were significantly higher than those in the YC group. The expression of Bcl-2 showed an opposite trend. Furthermore, the mRNA levels were decreased significantly after aerobic endurance exercise. Inflammation has been closely related to apoptosis, which is acknowledged to play a crucial role in the pathogenesis of inflammatory diseases (Oyinloye *et al.*, 2015). We found that aerobic endurance exercise significantly downregulated the mRNA expression levels of IL-6. In addition, the protein levels of Cleaved-Caspase 3 in the OC group were significantly higher than those in the YC group. After aerobic endurance exercise, the protein levels decreased significantly. Together, these data suggest that aerobic endurance exercise improves aging of renal vessels in the elderly and is closely related to apoptosis of vascular endothelial cells.

Studies have illustrated that the PI3K/AKT/mTOR pathway is generally considered to be the key signaling pathway to control metabolism and oxidative stress, involvement in angiogenesis, and regulation of endothelial cell apoptosis (Gerber *et al.*, 1998; Cheng *et al.*, 2017). To date, accumulating data from biological studies demonstrated that the P13K/AKT/mTOR pathway plays a prominent role in cell survival, metabolism, growth, and proliferation by directly regulating apoptotic proteins, such as Bcl-2, caspase-3, and Bax (Pathania *et al.*, 2013; Hui *et al.*, 2014). In the present study, the immunofluorescence analysis of p-AKT and p-mTOR indicated that numerous positive signals were present in glomerulus of the OC group. However, in the YC group, limited positive signals were observed in glomerulus. The results of the western blot analysis indicated that the levels of PI3K, phosphorylated AKT, and mTOR in the OC group were significantly higher than those in the YC group. Furthermore, the levels were decreased after aerobic

endurance exercise. Given these findings, we infer that aerobic endurance exercise improves vascular aging in aged kidney tissue and is closely related to the PI3K/AKT/mTOR signaling pathway. The expression of phosphorylated AKT and mTOR may inhibit the release of Bax, as well as other downstream pro-apoptotic protein caspases, resulting in the lower levels of apoptotic cells in the OY group.

In conclusion, the results of the present study suggested that the aging of glomerular vessels in aged kidney tissues is closely linked to the apoptosis of vascular endothelial cells. Aerobic endurance exercise, as an important rehabilitation intervention, significantly inhibited the decrease in senescence and apoptosis and enhanced the PI3K/AKT/mTOR activation, thereby improving the renal vascular sclerosis caused by aging. The present findings provided a novel approach for the prevention and treatment of aerobic exercise in the elderly patients with renal vascular sclerosis.

Authors' Contributions

H.L. and B.S. conceived and designed the experiments. C.B. performed the experiments. Z.Y. collected the data. Q.L. and C.B. analyzed the data. Q.C. prepared the figures. Z.Y. edited and revised the article. All authors reviewed and approved the final version of the article.

Disclosure Statement

No competing financial interests exist.

Funding Information

This work was financially supported by the National Natural Science Foundation of China grants (31500969 and 31471148).

References

Arida, A., Protogerou, A.D., Kitas, G.D., and Sfikakis, P.P. (2018). Systemic inflammatory response and atherosclerosis: the paradigm of chronic inflammatory rheumatic diseases. Int J Mol Sci **19,** 1890.

Banks, L, Buchan, T.A., Dizonno V. (2016). Aerobic exercise attenuates ageing of the athletic heart. J Physiol **594,** 3183–3184.

Barton, M. (2014). Aging and endothelin: determinants of disease. Life Sci **118,** 97–109.

Bellafiore, M., Sivverini, G., Palumbo, D., Macaluso, F., Bianco, A., Palma, A., *et al.* (2007). Increased cx43 and angiogenesis in exercised mouse hearts. Int J Sports Med **28,** 749–755.

Bhayadia, R., Schmidt, B.M., Melk, A., and Hömme, M. (2016). Senescence-induced oxidative stress causes endothelial dysfunction. J Gerontol **71,** 161.

Brodsky, S.V., Olga, G., Jun, C., Fan, Z., Nobuhiko, T., Mark, C., *et al.* (2004). Prevention and reversal of premature endothelial cell senescence and vasculopathy in obesity-induced diabetes by ebselen. Circ Res **94,** 377–384.

Cai, Q., Yao, Z., and Li, H. (2014). Catalpol promotes oligodendrocyte survival and oligodendrocyte progenitor differentiation via the Akt signaling pathway in rats with chronic cerebral hypoperfusion. Brain Res **1560,** 27–35.

Chen, K., Wang, N., Diao, Y., Dong, W., Sun, Y., Liu, L., *et al.* (2017). Hydrogen-rich saline attenuates brain injury induced by cardiopulmonary bypass and inhibits microvascular endothelial cell apoptosis via the PI3K/Akt/GSK3β signaling pathway in rats. Cell Physiol Biochem **43,** 1634–1647.

Cheng, H.W., Chen, Y.F., Wong, J.M., Weng, C.W., Chen, H.Y., Yu, S.L., *et al.* (2017). Cancer cells increase endothelial cell tube formation and survival by activating the PI3K/Akt signalling pathway. J Exp Clin Cancer Res **36**, 27.

Chimenti, L., Morici, G.A., Bonanno, A., Siena, L., Licciardi, A., Veca, M., *et al.* (2007). Endurance training damages small airway epithelium in mice. Am J Respir Crit Care Med **175,** 442–449.

Collett, J.A., Mehrotra, P., Crone, A., Christopher, S.W., Yoder, M.C., and Basile, D.P. (2017). Endothelial colony forming cells ameliorate endothelial dysfunction via secreted factors following ischemia-reperfusion injury. Am J Physiol Renal Physiol **312,** F897.

de Bragança, A.C., Canale, D., Gonçalves, J.G., Shimizu, M.H.M., Seguro, A.C., and Volpini, R.A. (2018). Vitamin D deficiency aggravates the renal features of moderate chronic kidney disease in 5/6 nephrectomized rats. Front Med (Lausanne) **5,** 282.

Del, P.F., Mariotti, A., Ilardi, M., Messina, F.R., Afeltra, A., and Amoroso, A. (1999). Kidney vasculogenesis and angiogenesis: role of vascular endothelial growth factor. Eur Rev Med Pharmacol Sci **3,** 149–153.

Denic, A., Glassock, R.J., and Rule, A.D. (2016). Structural and functional changes with the aging kidney. Adv Chronic Kidney Dis **23,** 19–28.

Ferrara, N., Gerber, H.P., and LeCouter, J. (2001). The role of vascular endothelial growth factor in angiogenesis. Acta Haematol **106,** 148–156.

Ferrara, N., Gerber, H.P., and LeCouter, J. (2003). The biology of VEGF and its receptors. Nat Med **9,** 669–676.

Garatachea, N., Pareja-Galeano, H., Sanchis-Gomar, F., Santos-Lozano, A., Fiuza-Luces, C., Morán, M., *et al.* (2015). Exercise attenuates the major hallmarks of aging. Rejuvenation Res **18,** 57–89.

Gerber, H.P., Mcmurtrey, A., Kowalski, J., Yan, M., Keyt, B.A., Dixit, V., *et al.* (1998). Vascular endothelial growth factor regulates endothelial cell survival through the phosphatidylinositol 3′-kinase/Akt signal transduction pathway. Requirement for Flk-1/KDR activation. J Biol Chem **273,** 30336–30343.

Ghosh, A., Gao, L., Thakur, A., Siu, P.M., and Lai, C.W.K. (2017). Role of free fatty acids in endothelial dysfunction. J Biom Sci **24,** 50.

Glassock, R.J., and Rule, A.D. (2012). The implications of anatomical and functional changes of the aging kidney: with an emphasis on the glomeruli. Kidney Int **82,** 270–277.

Gliemann, L., Rytter, N., Piil, P., Nilton, J., Lind, T., Nyberg, M., *et al.* (2018). The endothelial mechanotransduction protein platelet endothelial cell adhesion molecule-1 is influenced by aging and exercise training in human skeletal muscle. Front Physiol **18,** 1807.

Hommos, M.S., Glassock, R.J., and Rule, A.D. (2017). Structural and functional changes in human kidneys with healthy aging. J Am Soc Nephrol **28,** 2838–2844.

Hui, G., Hui, W., and Jianjun, P. (2014). Hispidulin induces apoptosis through mitochondrial dysfunction and inhibition of P13k/Akt signalling pathway in HepG2 cancer cells. Cell Biochem Biophys **69,** 27–34.

Ji, N., Luan, J., Hu, F., Zhao, Y., Lv, B., Wang, W. *et al.* (2018). Aerobic exercise-stimulated Klotho upregulation extends life span by attenuating the excess production of reactive oxygen species in the brain and kidney. Exp Ther Med **16,** 3511–3517.

Karar, J., and Maity, A. (2011). PI3K/AKT/mTOR Pathway in Angiogenesis. Front Mol Neurosci **2,** 51.

Li, P., Ma, L.L., Xie, R.J., Xie, Y.S., Wei, R.B., Yin, M., *et al.* (2012). Treatment of 5/6 nephrectomy rats with sulodexide: a novel therapy for chronic renal failure. Acta Pharmacol Sin **33,** 644–651.

Majumder, S., and Advani, A. (2016). VEGF and the diabetic kidney: more than too much of a good thing. J Diabetes Complications **31,** 273–279.

Marcaletti, S., Thomas, C., and Feige, J.N. (2011). Exercise performance tests in mice. Curr Protoc Mouse Biol **1,** 141–154.

Martens, C.R., Kirkman, D.L., and Edwards, D.G. (2016). The Vascular Endothelium in Chronic Kidney Disease: A Novel Target for Aerobic Exerc Sport Sci Rev **44,** 12–9.

Nyberg, M., Blackwell, J.R., Damsgaard, R., Jones, A.M., Hellsten, Y., and Mortensen, S.P. (2012). Lifelong physical activity prevents an age-related reduction in arterial and skeletal muscle nitric oxide bioavailability in humans. J Physiol **590,** 5361–5370.

Osullivan, E.D., Hughes, J., and Ferenbach, D.A. (2017). Renal aging: causes and consequences. J Am Soc Nephrol **28,** 407–420.

Oyinloye, B.E., Adenowo, A.F., and Kappo, A.P. (2015). Reactive oxygen species, apoptosis, antimicrobial peptides and human inflammatory diseases. Pharmaceuticals **8,** 151.

Papazova, D.A., Krebber, M.M., Oosterhuis, N.R., Gremmels, H., van Zuilen, A.D., Joles, J.A., *et al.* (2018). Dissecting recipient from donor contribution in experimental kidney transplantation: focus on endothelial proliferation and inflammation. Dis Models Mech **11,** dmm035030.

Pathania, A.S., Guru, S.K., Verma, M.K., Sharma, C., Abdullah, S.T., Malik, F., *et al.* (2013). Disruption of the PI3-K/AKT/mTOR signaling cascade and induction of apoptosis in HL-60 cells by an essential oil from *Monarda citriodora*. Food Chem Toxicol **62,** 246–254.

Pope, C.A., Bhatnagar, A., McCracken, J., Abplanalp, W.T., Conklin, D.J., and O'Toole, T.E. (2016). Exposure to fine particulate air pollution is associated with endothelial injury and systemic inflammation. Circ Res **119,** 1204–1214.

Roof, S.R., Ho, H., Little, S.C., Ostler, J.E., Brundage, E.A., Periasamy, M., *et al.* (2015). Obligatory role of neuronal nitric oxide synthase in the heart's antioxidant adaptation with exercise. J Mol Cell Cardiol **81,** 54–61.

Rzechorzek, W., Zhang, H., Buckley, B.K., Hua, K., Pomp, D., and Faber, J.E. (2017). Aerobic exercise prevents rarefaction of pial collaterals and increased stroke severity that occur with aging. J Cereb Blood Flow Metab **37,** 3544–3545.

Satoh, M., Kidokoro, K., Ozeki, M., Nagasu, H., Nishi, Y., Ihoriya, C., *et al.* (2013). Angiostatin production increases in response to decreased nitric oxide in aging rat kidney. Lab Invest **93,** 334–343.

Schnell, C.R., Staquffer, F., Allegrini, P.R., O'Reilly, T., Mcsheehy, P.M., Dartois, C., *et al.* (2008). Effects of the dual phosphatidylinositol 3-kinase/mammalian target of rapamycin inhibitor NVP-BEZ235 on the tumor vasculature: implications for clinical imaging. Cancer Res **68,** 6598–6607.

Shao, Y., Wolf, P., Guo, S., Guo, Y., Gaskins, H.R., and Zhang, B. (2017). Zinc enhances intestinal epithelial barrier function through the PI3K/AKT/mTOR signaling pathway in Caco-2 cells. J Nutr Biochem **43,** 18–26.

Tian, X., Shi, Y., Liu, N., Yan, Y., Li, T., Hua, P., *et al.* (2016). Upregulation of DAPK contributes to homocysteine-induced endothelial apoptosis via the modulation of Bcl2/Bax and activation of caspase 3. Mol Med Rep **14,** 4173–4179.

Viña, J., Rodriguez-Mañas, L., Salvador-Pascual, A., Tarazona-Santabalbina, F.J., and Gomez-Cabrera, M.C. (2016). Exercise: the lifelong supplement for healthy ageing and slowing down the onset of frailty. J Physiol **594,** 1989–1999.

Wang, F., Yamauchi, M., Muramatsu, M., Osawa, T., Tsuchida, R., and Shibuya, M. (2011). RACK1 regulates VEGF/Flt1-mediated cell migration via activation of a PI3K/Akt pathway. J Biol Chem **286,** 9097–9106.

Wang, H., Duan, L., Zou, Z., Li, H., Yuan, S., Chen, X., *et al.* (2014). Activation of the PI3K/Akt/mTOR/p70S6K pathway is involved in S100A4-induced viability and migration in colorectal cancer cells. Int J Med Sci **11,** 841–849.

Wu, R., Tang, S., Wang, M., Xu, X., Yao, C., Wang, S., *et al.* (2016). MicroRNA-497 induces apoptosis and suppresses proliferation via the Bcl-2/Bax-Caspase9-Caspase3 pathway and Cyclin D2 protein in HUVECs. PLoS One **11,** e0167052.

Yan, X., Hui, Y., Hua, Y., Huang, L., Wang, L., Peng, F., *et al.* (2019). EG-VEGF silencing inhibits cell proliferation and promotes cell apoptosis in pancreatic carcinoma via PI3K/AKT/mTOR signaling pathway. Biomed Pharmacother **109,** 762–769.

Ye, X., Cheng, S., Dong, Y., Ren, J., Su, L., Liu, J., *et al.* (2018). Exendin-4 promotes proliferation of adipose-derived stem cells through PI3K/Akt-Wnt signaling pathways. Neurosci Lett **15,** 196–202.

Yu, J., Wu, H., Liu, Z.Y., Zhu, Q., Shan, C., and Zhang, K.Q. (2017). Advanced glycation end products induce the apoptosis of and inflammation in mouse podocytes through CXCL9-mediated JAK2/STAT3 pathway activation. Int J Mol Med **40,** 1185–1193.

Yuho, K., Triolo, M., and Hood, D.A. (2017). Impact of aging and exercise on mitochondrial quality control in skeletal muscle. Oxid Med Cell Longev **2017,** 1–16.

Zhang, J., Xu, J., Dong, Y., and Huang, B. (2018). Downregulation of HIF-1α inhibits the proliferation, migration and invasion of gastric cancer by inhibiting PI3K/AKT pathway and VEGF expression. Biosci Rep **38,** DOI: 10.1042/BSR20180741.

Zhao, B., Quan, H., Ma, T., Tian, Y., Cai, Q., and Li, H. (2015). 4,4′-diisothiocyanostilbene-2,2′-disulfonic acid (DIDS) ameliorates ischemia-hypoxia-induced white matter damage in neonatal rats through inhibition of the voltage-gated chloride channel ClC-2. Int J Mol Sci **16,** 10457–10469.

Zhu, Y.B., Zhang, Y.P., Zhang, J., and Zhang, Y.B. (2016). Evaluation of vitamin C supplementation on kidney function and vascular reactivity following renal ischemic injury in mice. Kidney Blood Press Res **41,** 460–470.

Address correspondence to:
Bin Shu, PhD
Department of Rehabilitation Medicine
University-Town Hospital
Chongqing Medical University
Chongqing 401331
China

E-mail: BCCShu@163.com

Hongli Li, PhD
Department of Histology and Embryology
Army Medical University
Chongqing 400038
China

E-mail: lihongli@tmmu.edu.cn

Received for publication July 22, 2019; received in revised form November 17, 2019; accepted November 18, 2019.